Journal of Photonic Materials and Technology
2024, Vol. 10, No. 1, pp. 7-12
https://doi.org/10.11648/j.jmpt.20241001.12

Research Article

Influence of Graphene on Sheet Resistivity and Urbach Enery of Nano TiO_2 for DSSC Electrode

Geoffrey Gitonga Riungu[1, *], Simon Waweru Mugo[1], James Mbiyu Ngaruyia[1], Leonard Gitu[2]

[1]Department of Physics, College of Pure and Applied Sciences, Jomo Kenyatta University of Agriculture and Technology, Nairobi, Kenya

[2]Department of Chemistry, College of Pure and Applied Sciences, Jomo Kenyatta University of Agriculture and Technology, Nairobi, Kenya

Abstract

Importance of renewable energy cannot be over emphasized. Titanium IV oxide (TiO_2) is the most suitable semiconductor for dye sensitized solar cell (DSSC) due to its chemical stability, non toxicity and excellent optoelectronic properties. In this research TiO_2 is coated on graphene to enhance its charge transport aiming to reduce recombination which is a main set back in DSSCs. undestanding graphene- TiO_2 contact is therefore essential for DSSC application. TiO_2 thin films were deposited on single layer graphene (SLG) as well as on flourine tin oxide (FTO) using doctor blading technique. The films were annealed at rates of 2 ℃ /min and 1 ℃/min up to a temperature of 450 ℃ followed by sintering at this temperature for 30 minutes. Four point probe SRM-232 was used to measure sheet resistance of the samples. The film thickness were obtained from transmittance using pointwise unconstrained minimization approximation (PUMA). UV –VIS spectrophotometer was employed to measure transmittance. Resistivity of TiO_2 on both FTO and Graphene were of order 10^{-4} Ωcm. However, TiO_2 annealed on graphene matrix exhibited a slightly lower resistivity 5.6×10^{-4} Ωcm as compared to 6.0×10^{-4} Ωcm on FTO. Optical transmittance on visible region was lower for TiO_2 on FTO than on SLG, 71.48% and 80.11% respectively. Urbach energy (Eu) for weak absorption region decreased with annealing rate. Urbach energies for 1 ℃/min TiO_2 on FTO and SLG were 361 meV and 261meV respectively. This was used to account for decrease of disoders of films due to annealing. A striking relation between sheet resistivity and urbach was reported suggesting SLG as a suitable candidate for photoanode of a DSSC.

Keywords

Graphene, Urbach Energy, Resistivity, Annealing, Titanium IV Oxide

1. Introduction

Dye sensitized cells revolution is mainly based on titanium dioxide (TiO_2) films due to their excellent opto-electronic properties, such as high refractive index, large band gap and high transmittance in the visible region [1]. The optical and structural properties of TiO_2 films can be tailored for promoting its applications via deposition methods such as sputtering, doctor blading, chemical vapor deposition and sol–gel processes [2]. Doctor Blade is now a popular approach be-

*Corresponding author: geoffreyriungu@gmail.com (Geoffrey Gitonga Riungu)

Received: 15 June 2024; **Accepted:** 1 July 2024; **Published:** 23 July 2024

cause it is simple, easy to scale up, cost effective and suitable for a large area processing [3]. Several studies have been initiated to modify the electrical transport properties of TiO_2 using binary-system electrodes [4].

Graphene-based devices are auspicious candidates for future high-speed field-effect transistors (FETs), because they have a high carrier mobility of more than $10^4 cm^2V^{-1}s^{-1}$ [5]. The monolayer graphene is a zero-gap semiconductor with a linear dispersion, whereas the multilayer graphene is a semimetal with a small band overlap between the conduction and valence bands. Electrons through single layer graphene hop with minimal scattering and at very high Fermi velocity of $\sim 10^6 m/s$ [6].

The SRM-232 offers a low-cost hand held sheet resistance meter with four-point probe for use in measuring the sheet resistance of applied coatings such as conductive paints, EMI coatings, ITO on glass, and many other types of thin films.

Generally, in optical absorption, near band edges, an electron from the top of the valence band gets excited into the bottom of the conduction band across the energy band gap [7]. The Urbach energy indicating the width of the exponentially decaying sub-bandgap absorption tail is commonly used as the indicator of electronic quality of thin-film materials for application in solar cells [8].

In this work, analysis of electrical conductivity for TiO_2 grown on single layer grapheme (SLG) and the relationship to urbach energies is thus reported. This study is aimed at advancing the optoelectronic applications of SLG to dye sensitized solar cells.

2. Experimental Procedure

2.1. Materials

Single layer graphene was sourced from Charmgraphene Co.; Ltd, Gwonseon-gu, Suwon, Republic of Korea. Graphene films were synthesized with thermal chemical vapour deposition (CVD) technology based on the roll-to-roll method. SLG was coated on a SiO_2 substrate. Nanocrystalline TiO_2 (T/SP, 18% wt, sourced from Solaronix, Switzerland. FTO (SnO_2: F) 7 Ω/sq, was sourced from Xinyan Technology Co. Limited, China.

2.2. Thin Film Deposition and Annealing

Thin films were coated on FTO as well as on SLG using doctor blading technique. The prepared films were annealed using muffle furnace at controlled rates 1 ℃/min and 2 ℃/min from room temperature up to 450 ℃. the films were then sintered for 30 minutes the cooled gradually back to room temperature.

2.3. Measurements and Analysis

The optical transmittance was measured using double beam UV-Visible spectrophotometer (Shimadzu UV probe 1800, Japan) in the wavelength range of 200-1100 nm. Absorption coefficient Values of for all corresponding wavelengths were attained using SCOUT thin film analysis software analysis [9]. Sheet resistance of the films was measured using four-point probe, model SRM-232 as shown in figure 1.

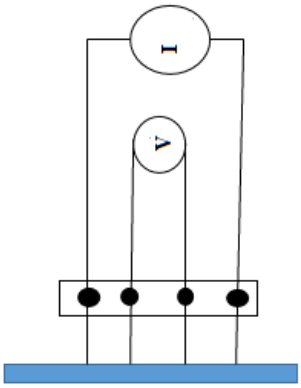

Figure 1. *Functional block diagram of SRM-232 Four-point probe.*

The voltage was measured across the inner probes while current was measured across the outer probes. The probes were operated manually by pressing to the film. Sheet resistance (R_S) values measured and displayed on the digital panel display. Resistivity (ρ) is defined in terms of voltage (V), current (I) and thickness (t) as in equation 1 and 2

$$\rho = 4.532 \frac{V}{I} t \tag{1}$$

$$\rho = 4.532 R_s t \ (\Omega\text{cm}) \tag{2}$$

The Urbach energy was calculated by plotting ln(α) vs. hv and fitting the linear part of the curve with a straight line. The gradient of the line was used to calculate the ubarch energies [10] as in equation 3

$$\alpha(h\nu) = \alpha_0 exp(\frac{h\nu}{E_u}) \tag{3}$$

A pointwise unconstrained optimization approach (PUMA) was used to estimate the thickness of the films from transmittance data [11]. Fora thin film deposited on a thick transparent substrate. The formulae giving thickness of film from the transmittance as a function of the wavelength λ is derived as shown [12] from equations 4-9:

$$\text{Transmittance (T)} = \frac{Ax}{B - Cx + Dx^2} \tag{4}$$

Where

$$A = 16s(n^2 + \kappa^2) \tag{5}$$

$$B = [(n+1)^2 + \kappa^2][(n+1)(n+s^2) + \kappa^2] \quad (6)$$

$$C = [(n^2 - 1 + \kappa^2)(n^2 - s^2 + \kappa^2) - 2\kappa^2(s^2 + 1)]2\cos\phi - \kappa[2(n^2 s^2 + \kappa^2) + (s^2 + 1)(n^2 - 1 + \kappa^2)]2\sin\phi \quad (7)$$

$$D = [(n-1)^2 + \kappa^2][(n-1)(n-s^2) + \kappa^2] \quad (8)$$

$$\phi = 4\pi nd/\lambda,\ x = \exp(-\alpha d),\ \alpha = 4\pi\kappa/\lambda. \quad (9)$$

d is the thickness of the film, s and n are the index of refraction of the substrate and of the film respectively, α is the absorption coefficient and κ is the (dimensionless) extinction coefficient.

3. Results and Discussion

3.1. Sheet Resistance

Figure 2 shows sheet resistance for annealed TiO_2 on fluorine doped tin IV oxide (FTO) and single layer graphene (SLG).

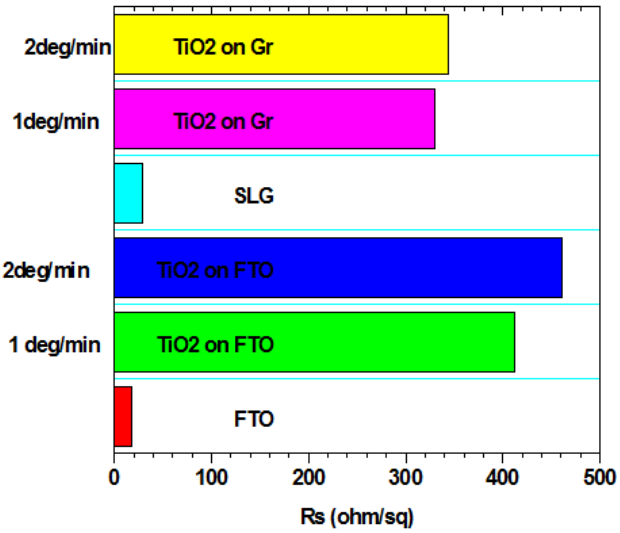

Figure 2. *Sheet resistance for annealed TiO_2 on FTO and Graphene films.*

Sheet resistance of FTO is lower than SLG, 15.0 and 31.6 Ω/sq respectively. However, TiO_2 annealed on graphene substrate exhibited lower resistance than on FTO substrate, 3.28 x10^2 and 4.12 x 10^2 Ω/sq respectively. Mono layer graphene through its planar hexagonal lattice structure provides an increase in the layer conductivity for annealed TiO_2 resulting to better electron transport for the composite film.

3.2. Sheet Resistivity

Figure 3 shows the sheet resistivity of TiO_2 as a function of annealing and effects of graphene on the resistivity.

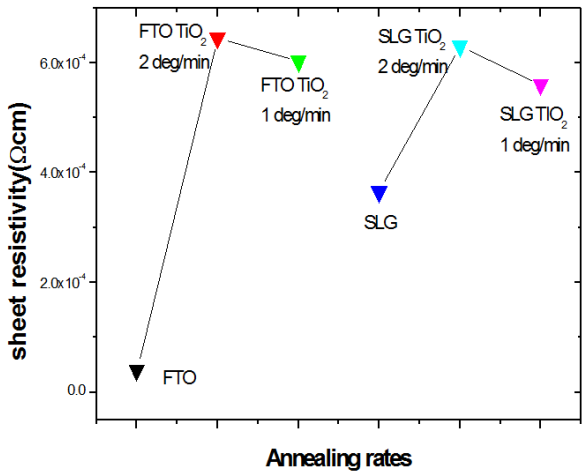

Figure 3. *Sheet resistivity against annealing for TiO_2 on FTO and grapheme.*

Sheet resistivity of TiO_2 on both FTO and Graphene were of order 10^{-4} Ωcm. however upon annealing TiO_2 at a rate of 1 ℃ per minute on SLG sheet resistivity is lower than on FTO. 5.6 x10^{-4} Ωcm is thus reported for SLG as compared to 6.0x10^{-4} Ωcm on FTO. FTO has uneven morphology [13] which results to high porosity of TiO_2 layer consequently producing subsurface defects in FTO/TiO_2 interface. On the other hand, graphene is highly crystalline. Therefore, this reduction in resistivity for TiO_2 annealed on graphene could be attributed better charge transport due decrease in lattice defects for TiO_2 annealed on graphene.

3.3. Transmittance

Figure 4 shows transmittance spectra for TiO_2 annealed on FTO and SLG. Graphene on glass had a transmittance peak at a wavelength of 502.89nm and a 81.62%. FTO on the other hand peaked at 746.43nm and 80.28% transmittance as shown in table 1.

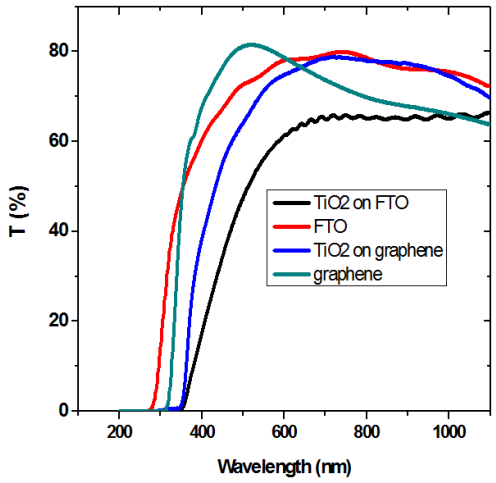

Figure 4. *Transmittance for annealed TiO_2 on graphene and FTO versus wavelength.*

For the annealed TiO_2 the peaks were at 686.71 nm and 754.22nm for SLG and FTO respectively. Transmittance for annealed films decreased more for FTO than Graphene 66.25% and 71.95% respectively.

Table 1. *Transmittance peaks for TiO_2 annealed on FTO and Graphene.*

Sample	Peak wavelength (λ) (nm)	Peak Transmittance (%)
Graphene	502.89	81.62
TiO_2 on Graphene	686.71	71.95
FTO	746.43	80.28
TiO_2 on FTO	754.22	66.25

High transmittance means that very few bonds of TiO_2 absorb a particular wavelength. Low transmittance implies there is a high number of TiO_2 bonds corresponding to vibrational energies of the incident wavelength. Thus their more absorption for TiO_2 on FTO than on Graphene. The peaks shift deeper in visible region as result of annealing as shown in table 1.

3.4. Absorption Coefficient

A graph of absorption coefficients against wavelength is shown in figure 5. The absorption is of order 10^4 for all samples.

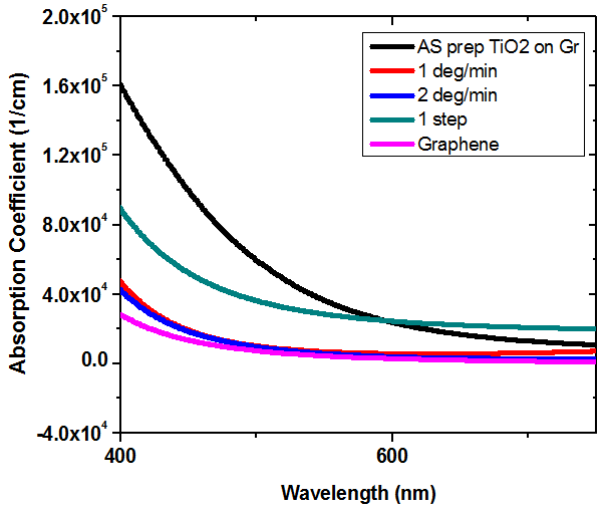

Figure 5. *Absorption coefficient for as deposited and annealed TiO_2 films on Graphene.*

The coefficients decrease exponentially for all samples within the visible region. This indicates presence of localized states in band gap. The absorption edge can be used to give a measure of the energy bandgap. The dependence of the absorption coefficient was used to to evaluate Urbach energies using Urbach rule as in equation 3.

3.5. Urbach Energy for TiO_2 on Graphene and FTO

Figure 6 shows the dependence of absorption coefficient edges tailing in weak absorption region (W), urbach region (U) optical transitions from extended state (T). Tailing of ρ(hν) extending into the energy band gap in region W is observed for TiO_2 on graphene and FTO. The tailing is more pronounced for TiO_2 on FTO than on graphene.

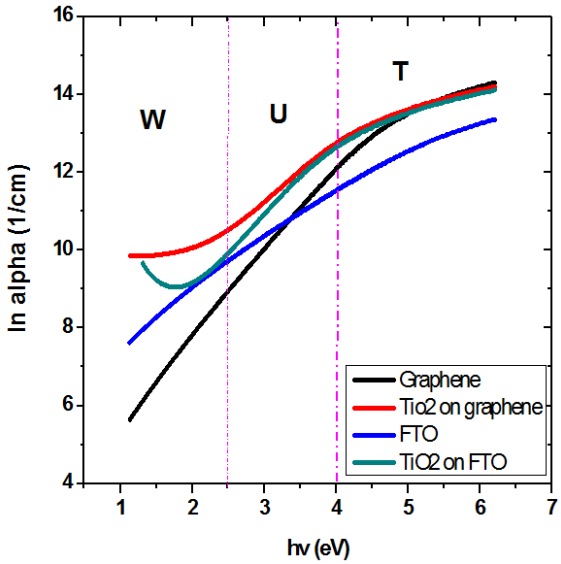

Figure 6. *ln (α) vs (hυ) for annealed TiO_2 on Graphene and FTO.*

Exponential tails are associated with low crystalline films, and disordered amorphous materials because of localized states [14, 15]. Further, tailing of bands is associated to lattice vibration due creation of sub-surface defects such as vacancy-interstitial pairs and antisites [16]. Therefore, this tailing implies presence of more localized states in band gap for TiO_2 coated on FTO than on graphene. Absence of tailing for graphene and FTO signifies minimal or no localized states. In order to quantify the broadness of the density of states Ubarch energies were evaluated using equation 3. The Urbach Energy enumerates the steepness of the onset of absorption near the band edge.

Table 2. *Urbach energies of TiO_2 on FTO and graphene.*

Urbach energy	2^o/ min	1^o/min
Tio_2 on FTO Eu (meV)	414	365
TiO_2 on Graphene(meV)	329	260

Evaluated Urbach energies of TiO_2 films on FTO were higher than SLG *as* shown in table 2. High Urbach energy confirms enhanced photocatalytic efficiency due to the disorder and defects that introduced localized states at or near the conduction band level [17]. Therefore, lower urbach energies 260 meV signifies less lattice defects for TiO_2 on SLG substrate.

3.6. Relationship of Urbach Energy and Resistivity of TiO_2 on Graphene and FTO

We observe from figure 7 a direct variation between Urbach energy and sheet resistivity of TiO_2 on FTO as well as on SLG. The optical band gap, Urbach energy, and electrical resistivity were found to have systematic dependence on the crystallite size [18] In low crystalline, weakly crystalline, disordered, and amorphous materials, there exists an exponential tail at the band edge of the absorption/absorption coefficient curve known as the Urbach tail. This exponential tail plays a crucial role in understanding the electronic transport properties of composite materials [19].

Therefore, as observed in figure 7, TiO_2 annealed films on graphene have a lower urbach energy as well as sheet resistivity 260meV and 5.6 $x10^{-4}$ Ωcm. Annealing gradually increases crystallite sizes, decreases lattice imperfections as well as enhancing nucleation and coalescence. However, from studies by [20] localized tail states in amorphous semiconductors have been reported to arise from defects generated disorder. The decrease in resistivity of TiO_2 on SLG can be attributed to good conductivity of graphene.

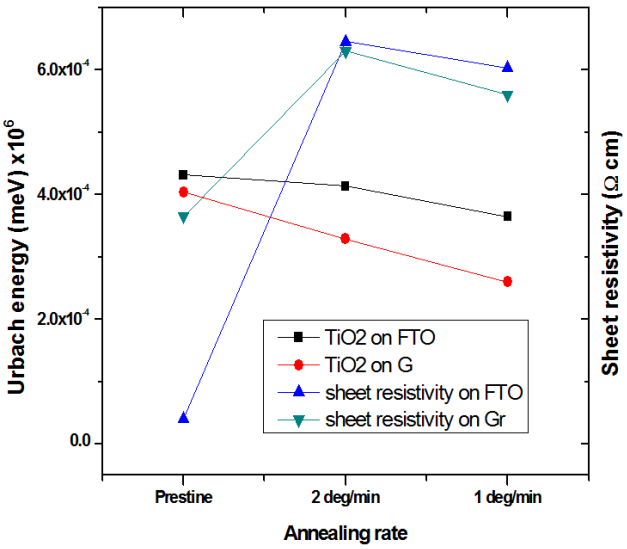

Figure 7. *A relation between Urbach energies and resistivity for TiO_2 on FTO and graphene.*

4. Conclusion

Uniform TiO_2 nanocomposite thin films were deposited on FTO as well as on graphene interface glass substrates using doctor blading deposition technique. The four-point probe, model SRM-232 was used to measure sheet resistance of the films. Sub-surface defects of the TiO_2 films on FTO and SLG as manifested by the Urbach energy tails in the band-gap were used as a measure of disorder of the films. A direct relation between Urbach energy and sheet resistivity as result of annealing is thus reported for both TiO_2 on FTO as well as on graphene. These observations indicate that a fine control over sheet resistivity and microstructure of the films can be achieved via annealing TiO_2 on graphene to harness it for various opto-electronic applications.

Acknowledgments

I would wish to acknowledge Jommo Kenyatta university of Agriculture and technology for the support accorded by physics, food science and chemistry laboratories in this study.

Abbreviations

FTO	Fourine Doped tin IV Oxide
SLG	Single Layer Grapheme
Gr	Grapheme
1deg/min	One Degree Per Minute
2deg/min	Two Degrees Per Minute
Eu	Urbach Energy
TiO_2	Titanium IV Oxide
CVD	Chemical Vapour Deposition

Author Contributions

Geoffrey Gitonga Riungu: Conceptualization, Data curation, Formal Analysis, Funding acquisition, Investigation, Methodology, Resources, Software, Writing – original draft

Simon Waweru Mugo: Project administration, Resources, Supervision, Validation, Visualization, Writing – review & editing

James Mbiyu Ngaruyia: Supervision, Validation, Visualization, Writing – review & editing

Leonard Gitu: Supervision

Conflicts of Interest

The authors declare no conflicts of interest.

References

[1] Fuyuki T, Matsunami H. Electronic properties of the interface between Si and TiO_2 deposited at very low temperatures. Jpn J Appl Phys 1986; 25: 1288. https://doi.org/10.1143/JJAP.25.1288

[2] Miao L Et al. Preparation and characterization of polycrystalline anatase and rutile TiO_2 thin films by rf magnetron sputtering. Appl Surf Sci 2003; 212: 255. https://doi.org/10.1016/S0169-4332(03)00106-5

[3] Benjamin M. J., Simon W. M., and James M. N. (2018) "Effect of Annealing Rates on Surface Roughness of TiO_2 Thin films." Journal of Materials Physics and Chemistry, 6(2): 43-46.

[4] R. Jose, V. Thavasi, and S. Ramakrishna, "Metal oxides for dye-sensitized solar cells," Journal of the American Ceramic Society, vol. 92 (2), pp. 289-301, 2009. https://doi.org/10.1111/j.1551-2916.2008.02870.x

[5] Geim, A. K., & Novoselov, K. S. (2007). The rise of graphene. Nature materials, 6(3), 183-191.

[6] K. S. Novoselov, A. K. Geim, S. V. Morozov, D. Jiang, Y. Zhang, S. V. Dubonos, I. V. Grigorieva, and A. A. Firsov, Electric field effect in atomically thin carbon films, *Science*, *306*, 2004, 666–669. https://doi.org/10.1126/science.1102896

[7] Boubaker, K. A physical explanation to the controversial Urbach tailing universality. Eur. Phys. J. Plus 126, 10 (2011). https://doi.org/10.1140/epjp/i2011-11010-4

[8] Biwas Subedi, Chongwen Li, Cong Chen, Dachang Liu, Maxwell M. Junda, Zhaoning Song, Yanfa Yan, and Nikolas J. PodrazaACS Applied Materials & Interfaces 2022 14 (6), 7796-7804. https://doi.org/10.1021/acsami.3c01849

[9] Theiss, W. (2000). Scout thin films analysis software handbook, edited by Theiss M (Hand and Software Aachen German) www.mtheiss.com

[10] Boubaker K. (2011). A physical explanation to the controversial Urbach tailing universality, The European Physics Journal Plus, 126, 10.

[11] Ernesto G. Birgin, Ivan E. Chambouleyron, José Mario Martínez, Sergio D. Ventura, Estimation of optical parameters of very thin films, Applied Numerical Mathematics, 47, 2003, 109-119. https://doi.org/10.1016/S0168-9274(03)00055-2

[12] Ernesto G Birgin, Ivan Chambouleyron, José Mario Martínez, Estimation of the Optical Constants and the Thickness of Thin Films Using Unconstrained Optimization, Journal of Computational (1999) Physics, 151: 862880. https://doi.org/10.1006/jcph.1999.6224

[13] Larbah, Youssef & Rahal, Badis & Adnane, Mohamed. (2020).The effect of fluorine doping on the properties of SnO_2 thin films deposited using spray pyrolysis method. Journal of Optoelectronics and Advanced Materials. 22. 518-522.

[14] El-Nahass, M. M., Soliman, H. S., El-Denglawey, A. (2016). Absorption edge shift, opticalconductivity, and energy loss function of nano thermal-evaporated N-typeanatase TiO_2 films. Appl Phys A; 122: 775.

[15] Mathews, N. R., Morales, E. R., Cortés-Jacome, M. A., & Antonio, J. T. (2009). TiO_2 thin films–Influence of annealing temperature on structural, optical and photocatalytic properties. Solar Energy, 83(9), 1499-1508. http://dx.doi.org/10.1016/j.solener.2009.04.008

[16] Wibowo, K. M., Sahdan, M. Z., Asmah, M. T., Saim, H., Adriyanto, F., & Hadi, S. (2017), August). Influence of Annealing Temperature on Surface Morphological and Electrical Properties of Aluminum Thin Film on Glass Substrate by Vacuum Thermal Evaporator. In IOP Conference Series: Materials Science and Engineering (Vol. 226, No. 1, p. 012180). IOP Publishing. http://dx.doi.org/10.1088/1757-899X/226/1/012180

[17] Jayasinghe, Lihini., Jayaweera, Vimukthi., de Silva, Nuwan., Mubarak, Azeez M. Role of ZrO2 in TiO_2 composites with rGO as an electron mediator to enhance the photocatalytic activity for the photodegradation of methylene blue. Materials Advances (2022) 3: 7904-7917. http://dx.doi.org/10.1039/D2MA00754A

[18] Dilawar Ali, M. Z. Butt, Iqra Muneer, FarooqBashir, MurtazaSaleem. Correlation between structural andoptoelectronic properties of tin doped indium oxide thin films (2017). 128: 235-246. https://doi.org/10.1016/j.ijleo.2016.10.028

[19] Rahman, Md. (2023). Synthesis of CdS and CdTe Through A Novel Solution Process for Application in Thin Film Solar Cells. https://www.researchgate.net/publication/373603736

[20] Al-Shomara, S. M., Alahmad W. R. (2019), Annealing temperature effect on structural, optical and photocatalytic activity of nanocrystalline TiO_2 films prepared by sol-gel method used for solar cell application, Digest Journal of Nanomaterials and Biostructures, 14, 617-625.